Accepted ms – Vadose Zone J. – doi: 10.2136/vzj2016.05.0039

# Spatial and Temporal Fluctuations of Pore-Gas Composition in Sulfidic Mine Waste Rock

Maria E. Lorca , K. Ulrich Mayer, Daniele Pedretti, Leslie Smith , Roger D. Beckie

University of British Columbia, Vancouver, BC, Canada

**Abstract**

Core Ideas

- Grain-size segregation during end dumping affects the pore-gas distribution.
- Seasonal variations in precipitation affect $O_2$ ingress and $CO_2$ egress.
- Hot spots of sulfide oxidation are controlled by physical and chemical heterogeneity.
- Grain-size segregation is reflected in the spatial distribution of oxidation rates.

The oxidation of sulfide minerals and pH-neutralization reactions in unsaturated mine waste rock produce changes in the pore-gas composition, leading to substantial deviations from atmospheric conditions. We studied the temporal and spatial changes in pore-gas composition, temperature, and volumetric water content (VWC) in an experimental pile during a 2-yr period. The pile was constructed by end dumping and is exposed to a marked two-season (wet–dry) climate. The grain-size segregation of waste rock occurring during end-dump construction significantly affected the spatial distribution of pore-gas composition within the pile. Results from continuous monitoring also demonstrated the role of VWC fluctuations on pore-gas composition at the study site. Oxygen decreased during the wet season, while $CO_2$ concentrations showed the opposite behavior. Gaseous diffusion was inferred as an important $O_2$ supply mechanism for this experimental waste-rock pile. In addition, wind-induced gas advection and convection probably contributed to $O_2$ ingress into the basal regions of the pile. Intrinsic oxidation rates were estimated based on one-dimensional reaction–diffusion modeling, showing pronounced variations between the top and bottom of the pile. These differences can be attributed to low reactivity in the basal region of the pile related to the coarse-grained nature of the material and the omission of $O_2$–supply mechanisms other than diffusion. The results demonstrate the complex interactions between physical and chemical heterogeneities in mine waste rock and contribute to an improved understanding of oxidation reactions and metal release that occur in sulfidic waste rock.

Abbreviations

- **TP**
- tipping phase
- **VWC**

volumetric water content

**Introduction**

Open-pit mining produces large amounts of waste rock containing variable amounts of sulfide minerals. This waste rock is deposited in storage facilities, under predominantly unsaturated conditions, where it can interact with water and $O_2$ derived from the atmosphere. Weathering of the sulfide minerals can lead to acid generation and metal release. The quality of the drainage depends strongly on the rate at which the sulfides are oxidized with time and the amount of pH-buffering minerals present in the system (**1**). Understanding the processes controlling metal release at the scale of operational facilities is required to make informed decisions for mine closure plans.

Oxidation of sulfide minerals in mine waste generates acidity, liberating metals and releasing sulfate, which negatively affects the quality of the drainage water. The oxidation reactions consume $O_2$ derived from the atmosphere, and the $O_2$ availability within the pile provides a major control on the progress and extent of sulfide mineral weathering. For example, the oxidation of pyrite can be described as

$$\mathrm{Fes}_2 + 3.5O_2 + H_2O \rightarrow 2H^+ + Fe^{2+} + 2SO_4^{2-} \quad (1)$$

Carbonate minerals, if present in the rock, neutralize acidity and release $CO_2$, which tends to partition into the gas phase. The dissolution of calcite can be written as

$$2\mathrm{H}^+ + \mathrm{CaCO}_3 \rightarrow \mathrm{CO}_2 + \mathrm{H}_2\mathrm{OCa}^{2+} \quad (2)$$

Oxygen consumption (Eq. [1]) and $CO_2$ generation (Eq. [2]) lead to characteristic changes in the pore-gas composition within waste-rock piles (12; 10). The resulting compositional differences in gas composition contribute to gas exchange between the waste-rock pile and the atmosphere.

Diffusion, advection, and convection are the most important mechanisms supplying $O_2$ to and releasing $CO_2$ from unsaturated mine waste materials (**24**; **35**). Gas concentration gradients cause diffusion, pressure differences trigger advection, and temperature variations produce convection. Pressure changes may be induced by atmospheric pumping (**35**), wind effects (**2**; **8**), or gas production and consumption (**22**). Monitoring the gas composition in space and time may reveal zones of enhanced reactivity and can provide information on the development of $O_2$-limited conditions. Exothermic sulfide mineral oxidation may increase internal temperatures, in some cases up to 50°C or higher (**15**; **24**), and drive convection that enhances the $O_2$ supply to the waste rock. Analysis of the pore-gas composition, together with temperature, provides information to characterize the contribution of the various transport mechanisms.

Irrespective of the transport mechanism, gas migration is affected by changes in the volumetric water content (VWC), for instance following precipitation events (e.g., **35**). Previous studies have indicated that precipitation patterns and the waste-rock water content have a

considerable influence on gas mobility and sulfide mineral weathering (**9**) and must be taken into consideration when studying gas migration and geochemical reactions in waste-rock piles.

To add further complexity, the pile internal VWC and reactivity are also affected by the grain size distribution of the waste rock. When waste-rock dumps are built by end dumping, grain segregation occurs, resulting in the preferential deposition of finer grained particles at the top and coarser particles at the bottom of the pile (e.g., **32**; **34**). This segregation can produce enhanced pathways for gas migration, in particular in the basal region (**35**), as well as variations in moisture retention capacity and reactivity.

Pore-gas composition in full-scale waste-rock dumps has been monitored in the past (**10**; **18**; **15**; **14**). Multilevel monitoring wells installed in operational or reclaimed dumps have provided depth-discrete information on pore-gas composition and related parameters (**17**; **33**). **2** and **8** studied the pore-gas composition and pressure within a 15-m-high experimental waste-rock pile. Pressure gradients within the pile responded to external wind speed, while $O_2$ and $CO_2$ concentrations remained near atmospheric levels, attributed to low sulfide mineral weathering rates and a high degree of gas mobility. However, to date, a study of gas compositional changes in an experimental pile with relatively reactive waste rock under a strong seasonal climate with pronounced wet and dry seasons has not been presented.

The goal of our work was to describe and analyze the results obtained from a 2-yr monitoring program focused on the analysis of the spatiotemporal evolution of VWC, temperature, and in particular pore-gas $O_2$ and $CO_2$ in an experimental waste-rock pile located in northern Peru. The pile is 10 m high, was built by end dumping, and is composed of potentially acid-generating intrusive rocks. Our study was designed to address the following research questions:

1. How does a two-season (wet–dry) climate affect the internal pore-gas composition of the pile?
2. Does particle-size segregation found in end-dumped piles have a significant effect on the internal gas composition?
3. What can be learned from the pore-gas composition to assess physical and chemical heterogeneity within the waste-rock pile?
4. Based on temperature and gas compositional data, which transport processes control the migration of $O_2$ and $CO_2$ within the pile?
5. How well can intrinsic oxidation rates within the experimental waste-rock pile be determined from the observed gas compositional data?

## Materials and Methods

The study site is located at a Cu–Zn mine in the High Andes of Peru. The mine is one of the largest polymetallic skarn deposits in the world, producing substantial volumes of waste rock, which is placed by end

dumping in piles up to 300 m high. Two distinct seasons occur at the site: a rainy season, which lasts from October to April, and a dry season between May and September. Ambient air temperatures at the site do not vary significantly during the year. The average air temperature during the dry season is $T$ = 5.1°C, while the average air temperature during the wet season is $T$ = 4.9°C, determined based on a data set ranging from February 2011 to April 2012 collected directly at the study site during the study period.

Total yearly rainfall at the site averages approximately 1300 mm $yr^{-1}$. Precipitation was measured on site with a Campbell Scientific rain gauge. In August 2011, this site rain gauge failed, and precipitation data thereafter were obtained from a nearby weather station (located about 4 km away and at 200 m lower elevation). Analysis of historical data has shown that precipitation patterns at the weather station site are similar to observations at the study site, implying that major rain events and seasonal dynamics at the site are well represented by the weather station data.

Five experimental piles were constructed at the site to provide insights into the processes occurring in the operational dumps. Pile 2, the focus of this study, is composed of relatively fine-grained intrusive material with substantial sulfide content and represents the most reactive of the five experimental piles (**26**). The pile was built in late 2007 to 2008. A bituminous geomembrane (Coletanche NPT4) with a hydraulic conductivity (for water) of $1 \times 10^{-11}$ m $s^{-1}$ or less at the base allows the collection of all water infiltrating through the crest and batters of the pile.

The experimental pile (36 m long by 36 m wide by 10 m high) contains approximately 24,000 Mg of waste rock and has a volume of about 12,000 $m^3$. The pile was built in four tipping phases (TP): first, a protective layer was installed across the base of the pile (TP 0); subsequently, the pile was constructed by placing three, distinct end-dumped waste-rock discharges (TP 1–3). The elemental composition, the ratio of neutralization potential to acid generation potential, and the grain-size distribution of the rock vary significantly among the discharges and are shown in **Table 1** (modified from **26**). Materials emplaced during discharge of TP 3 and TP 1B are finer grained than the waste rock from discharge of TP 1A and TP 2. Also, the S content of TP 3 and TP 1B are above average for the pile. Smaller scale field-barrel weathering experiments demonstrated that the rock of TP 3 is the most reactive (i.e., indicated by elevated $SO_4$ release, higher $O_2$ consumption rates, and lower pH in the outflow) compared with the other pile materials (**25**). The hydraulic conductivity of the pile varies with depth. Ring infiltrometer tests performed on the traffic surface at the top of the pile yielded values ranging from $5 \times 10^{-8}$ to $5 \times 10^{-5}$ m $s^{-1}$, with an average value of $1 \times 10^{-5}$ m $s^{-1}$ (**25**). Water balance modeling yielded an average saturated hydraulic conductivity of $6 \times 10^{-4}$ m $s^{-1}$ (**11**), indicative of higher hydraulic conductivities in the lower portion of the pile below the traffic surface.

**Table 1.** Selected results for the constructed pile materials. Sulfate release rate (mg $kg^{-1}$ $wk^{-1}$) for the corresponding field barrel () and corresponding oxygen consumption rates.

| Tipping phase | NP/AP† | S | C‡ | $SO_4$ release rate | $S_o$§ | Grain size analysis¶ | | |
|---|---|---|---|---|---|---|---|---|
| | | | | | | $D_{10}$ | $D_{50}$ | $D_{90}$ |
| | | % (w/w) | | mg $kg^{-1}$ $wk^{-1}$ | kg $m^{-3}$ $s^{-1}$ | mm | | |
| Protective layer | 1.49 | 0.62 | 0.17 | 5.0 ± 4.9# | 7.7 ± 7.6 × $10^{-9}$ | 1 | 30 | 100 |
| TP 1a | 1.90 | 0.20 | 0.15 | 1.4 ± 1.1 | 2.2 ± 1.7 × $10^{-9}$ | 0.15 | 30 | 75 |
| TP 1b | 0.06 | 4.26 | 0.09 | 28.7 ± 24.0 | 4.4 ± 3.7 × $10^{-8}$ | <0.1 | 9 | 60 |
| TP 2 | 0.40 | 0.64 | 0.08 | 3.6 ± 3.3 | 5.6 ± 5.1 × $10^{-9}$ | 0.1 | 11 | 60 |
| TP 3 | 0.14 | 1.56 | 0.05 | 30.6 ± 39.4 | 4.7 ± 6.1 × $10^{-8}$ | 0.1 | 11 | 100 |

- † Neutralizing potential–acid producing potential ratio.
- ‡ From whole-rock analysis.
- § $O_2$ consumption rate corresponding to the specific $SO_4$ release rate.
- ¶ $D_X$ refers to grain size $x$ (mm) passing × percentage.
- # Mean ± 1 SD.

The phased construction allowed installation of six instrumentation lines above the protective layer and between the waste-rock discharges. Our focus in this study was on four instrumentation lines (1, 2, 4, and 6) located along a vertical cross-section through the center of the pile (**Fig. 1**). The instruments installed in the lines allow in situ measurement of temperature and VWC, as well as gas sampling. All instruments are connected to automated analysis and datalogging systems inside an instrumentation hut located adjacent to the pile.

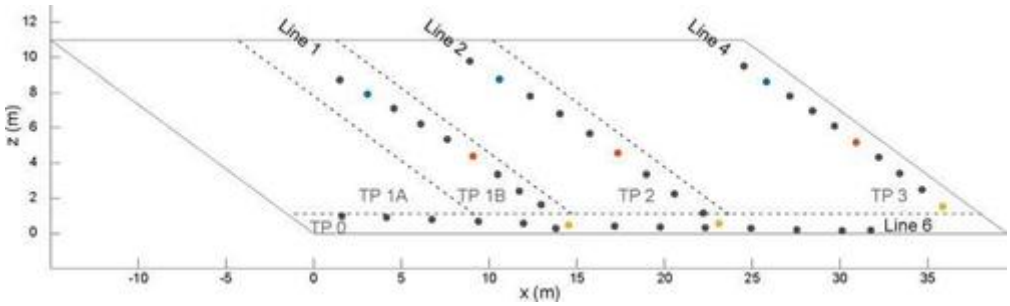


**Figure 1**

Location of protective layer TP 0 and end-dumped tipping phases (TP 1A, TP 1B, TP 2, and TP 3), instrumentation lines (Lines 1, 2, 4, and 6), and selected observation points for temporal data (top, blue; middle, red; bottom, orange).

Seventeen $ECH_2O$-TE probes (Decagon Devices) were installed along the four instrumentation lines selected for this study (**Fig. 1**). The TE probes measure VWC, electrical conductivity (not shown here), and temperature. The TE probes were calibrated according to the manufacturer's specifications, providing an accuracy of approximately ±3% for most mineral soils. Thermal and electrical conductivity effects were neglected for the water content measurements. Additional internal temperature measurements were obtained with five thermistors (RST Instruments). The TE probe and thermistor measurements were automated to collect measurements at 30-min intervals using a Campbell Scientific datalogger (CR 1000). Temperature data from the TE probes and thermistors installed in close proximity were consistent. Additional details about sensor installation and measurement techniques were provided by **4**.

An automated gas analysis system was used to measure $O_2$ and $CO_2$ composition from 64 monitoring ports (**31**); 43 of these ports are located along the vertical cross-section examined in this study. An array of solenoids was used to connect the gas ports in the pile to a peristaltic pump that conveyed the gas to $CO_2$ and $O_2$ analyzers with a flow rate of 300 mL $min^{-1}$. After the pump and before passing by the sensors, the gas stream was conditioned with a Genie Model 120 filter designed to remove moisture to optimize measurement accuracy and avoid damage to the sensors. The filter removed the moisture together with about 30% of the flow, the remainder of which was delivered to the sensors. Carbon dioxide concentrations were measured with a LI-820 (Li-Cor Biosciences) infrared gas analyzer, and $O_2$ content was measured using a SO-200 (Apogee Instruments) galvanic $O_2$ sensor with a flow-through head. Both instruments and the solenoid arrays were controlled by a CR1000 (Campbell Scientific) datalogger. The $CO_2$ analyzer measured in the range of 0 to 2% (v/v). The $O_2$ analyzer covered a range from 0 to 100%.

During a period of 2 yr (June 2010–May 2012), this automated system was used daily to analyze $CO_2$ and $O_2$ samples collected from each port. Pore gas was analyzed after purging for 2 min to ensure that the samples were representative of conditions within the pile. The combined time for purging and analysis amounted to 3 min per port, allowing the completion of a round of measurements during 3 h. The purge time lasted 2 min and was determined based on the internal line volume of the longest line in

the pile and the measured pumping rate. A safety factor of 2 was applied to ensure that purging was complete. Measurements were taken every 3 s during the 1-min monitoring interval to document that readings had stabilized, and the last five readings were averaged to produce the reported values. Two ports were dedicated to gases of known reference concentrations, which were also analyzed daily to ensure that the instrumentation remained in working order and to facilitate post-measurement corrections of gas composition measurements, if necessary. These ports sampled air from outside the instrumentation hut ($3.8 \times 10^{-2}$% [v/v] $CO_2$, 20.95% [v/v] $O_2$) and a fixed-composition calibration gas (1.5% [v/v] $CO_2$, 98.5% [v/v] $N_2$, 0% [v/v] $O_2$). In general, the observations at these two ports accurately reflected the composition of the gas standards (standard deviations for air: $3.3 \times 10^{-3}$% (v/v) $CO_2$, 0.31% (v/v) $O_2$; for the calibration gas: $2.30 \times 10^{-2}$% [v/v] $CO_2$, $5.4 \times 10^{-2}$% [v/v] $O_2$) and remained stable during the measurement period of 2 yr, demonstrating the reliability of the gas analysis system. However, during the period between April and July 2011, the reference measurements intermittently deviated from the expected values (i.e., composition of the calibration gas). This time period corresponds to the end of the 2010–2011 wet season, and closer inspection of the sampling system revealed that the erroneous measurements were due to a temporary buildup of moisture in the gas-sampling tubing. As a result, data that were clearly affected by moisture buildup were removed from the data set. Nevertheless, this part of the data set had to be interpreted with caution. System operation resumed at normal operating mode near the end of the 2011 dry season. However, toward the end of the second year (2011–2012 wet season), a more substantial and permanent moisture buildup occurred, with visible water ingress in several of the gas-sampling tubes, which required the system to be disconnected and effectively terminated the automated gas measurements.

## Results

We analyzed data collected from two hydrological years (2010–2012), which corresponds to the time frame when the pH of the drainage from the pile changed from an initial value above 7 to <4, as described by **25**. To provide context, we briefly present an overview of the hydrological response of the pile, followed by a more detailed description of the gas composition based on the spatial distribution at two select times for wet and dry seasons. We then focus on the presentation of time series ($O_2$, $CO_2$, and temperature) from nine key locations within the pile.

The hydrological response of the experimental pile can be inferred from the evolution of VWC data, which records water content in the finer grained matrix material (**Fig. 2**). By 2010, Pile 2 had largely reached a state of dynamic equilibrium with the seasonal rainfall pattern. **Figure 2** shows the decline in VWC throughout the 2010 dry season and the quick rise in VWC with the onset of the wet season, which remained elevated until April to May, when the VWC displayed a slow recession behavior. During the dry seasons, the VWC generally continued to decline but also responded locally and temporarily to a few sporadic precipitation events. The timing of the response of each sensor to precipitation events as well as the minimum and maximum VWCs differed among the ports (**Fig. 2**).

Sensors located in the upper portion of the pile (top, blue lines; see **Fig. 1** for locations) displayed a quicker response to precipitation events and a larger amplitude than the sensors located deeper in the pile (middle, red lines; bottom, orange lines; see **Fig. 1** for locations). This behavior was expected and is commonly observed in unsaturated soils (e.g., **36**, **3**). A quick response to recharge was observed for all sensors located in the most external instrumentation line (L4) due to its location on the batter and the limited amount of waste rock located above these sensors. Although the VWC declined substantially during the dry season, there was continuous flow in the basal lysimeter, with rates decreasing most considerably toward the end of the dry season (**25**).

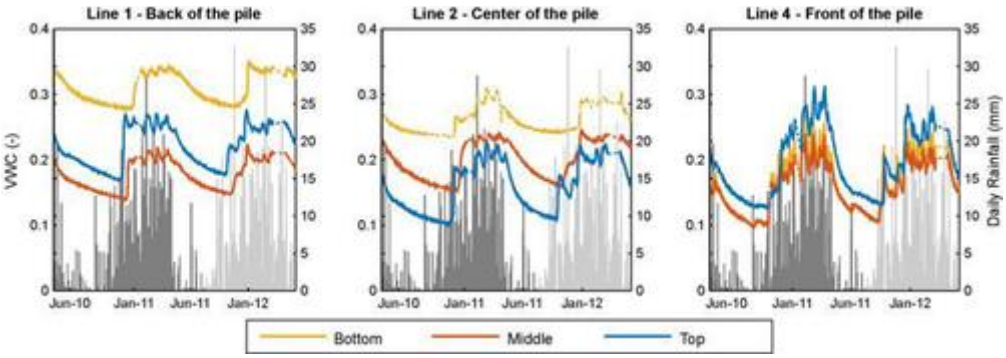


**Figure 2**

Evolution of volumetric water content (VWC) with time at selected locations in Instrumentation Lines 1, 2, and 4. Precipitation in the background: dark gray corresponds to data from the study site rain gauge; light gray corresponds to data from a weather station located 4 km away from the site.

Given the hydrological differences observed between the wet and dry seasons, two snapshots of the spatial distribution of $O_2$, $CO_2$, temperature, and VWC along the instrumentation lines are presented in **Fig. 3** and **4**. During both seasons, the pore-gas composition in the region near the top and front of the pile was significantly different from atmospheric conditions. During the dry season (**Fig. 3**), these deviations were most pronounced for $CO_2$ but can also be observed for $O_2$. Measured temperatures were highest near the front of the pile. Volumetric water content showed relatively dry conditions near the surface of the pile, with higher VWCs in the core and base of the pile. For wet season conditions (**Fig. 4**), elevated $CO_2$ concentrations above 1% (v/v) were observed along the entire top of the pile, extending from the front to the back of the pile. At this observation time, elevated $CO_2$ concentrations above 1% (v/v) were also observed in the basal regions near the front of the pile. The extent and magnitude of $O_2$ depletion was greater in the wet season than in the dry season. Measured temperatures during the wet season were generally lower than during the dry season, with the lowest temperatures measured near the pile surface. Notably, elevated temperatures near the front of the pile measured during the dry season were no longer observed during the wet season, when the change in VWC near the top of the pile was particularly pronounced.

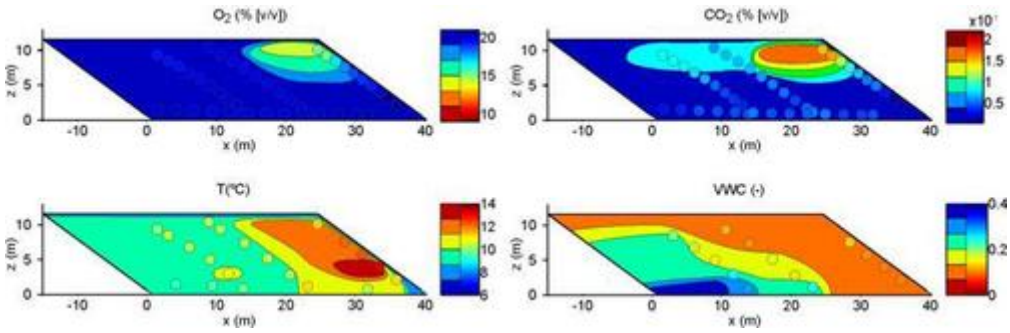


**Figure 3**

Spatial distribution of $O_2$, $CO_2$, temperature (*T*), and volumetric water content (VWC) at the end of the dry season (9 Oct. 2010). For gas composition, atmospheric composition is indicated by blue, while deviations from atmospheric composition are indicated by green to red; temperature increase is marked with red and average ambient temperature is blue; VWC corresponds to dry in red and wet in blue. Solid color bars correspond to contours, whereas graded color bars correspond to data points; contours are hand drawn.

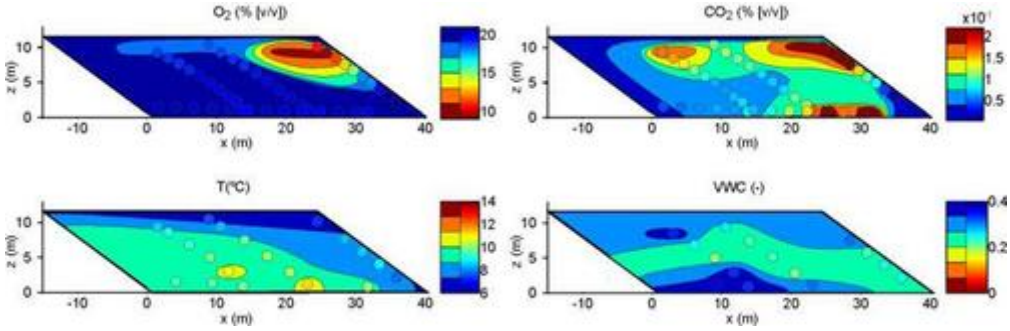


**Figure 4**

Spatial distribution of $O_2$, $CO_2$, temperature (*T*), and volumetric water content (VWC) at the end of the wet season (9 Mar. 2011). For gas composition, atmospheric composition is indicated by blue, while deviations from atmospheric composition are indicated by green to red; temperature increase is marked with red and average ambient temperature is blue; VWC corresponds to dry in red and wet in blue. Solid color bars correspond to contours, whereas graded color bars correspond to data points, contours are hand-drawn.

Closer examination of the data showed that substantial $O_2$ depletion occurred in the experimental pile. Concentrations of $O_2$ varied from atmospheric levels (20.95% v/v]) down to one-third of atmospheric $O_2$ content (7% [v/v]). The $CO_2$ concentrations ranged from atmospheric concentrations ($3.8\times 10^{-2}$% [v/v]) to >2% (v/v) (**Table 2**).

**Table 2.** Minimum and maximum of measured parameters (all monitoring points).

| Statistic | $CO_2$ | $O_2$ | Temperature | Volumetric water content |
|---|---|---|---|---|
| | % (v/v) | | °C | |

| Statistic | $CO_2$ | $O_2$ | Temperature | Volumetric water content |
|---|---|---|---|---|
| Min. | $3.8 \times 10^{-2}$ | 7 | 6.6 | 0.09 |
| Max. | >2 | 20.9 | 13.3 | 0.37 |

Time series of the observed gas concentrations (**Fig. 5**) confirm that during the wet season, $O_2$ depletion was most marked near the front of the pile (Line 4), with much lower observed $O_2$ depletions in the center and back of the pile (Lines 1 and 2). At the end of the dry season, $O_2$ concentrations remained depressed only near the front of the pile (Line 4), while $O_2$ contents measured toward the center and back of the pile (Lines 1 and 2) approached concentrations close to atmospheric. Within Line 1, the $O_2$ content was lower near the surface than in the middle and bottom ports, yet remained close to atmospheric conditions at all locations. The largest differences were observed between the top ports and the lower ports in the pile during the wet season. For the entire pile, the bottom port measurements remained above 20% (v/v), with small fluctuations between different daily measurements. Moisture accumulation in the sampling tubing toward the end of the 2010–2011 wet season probably contributed to the strong fluctuations in $O_2$ concentrations from April to July 2011, in particular because the $O_2$ sensor readings are sensitive to pressure changes. However, the observed concentration trends outside this time interval confirm the strong seasonal dependence of $O_2$ concentrations within the pile.

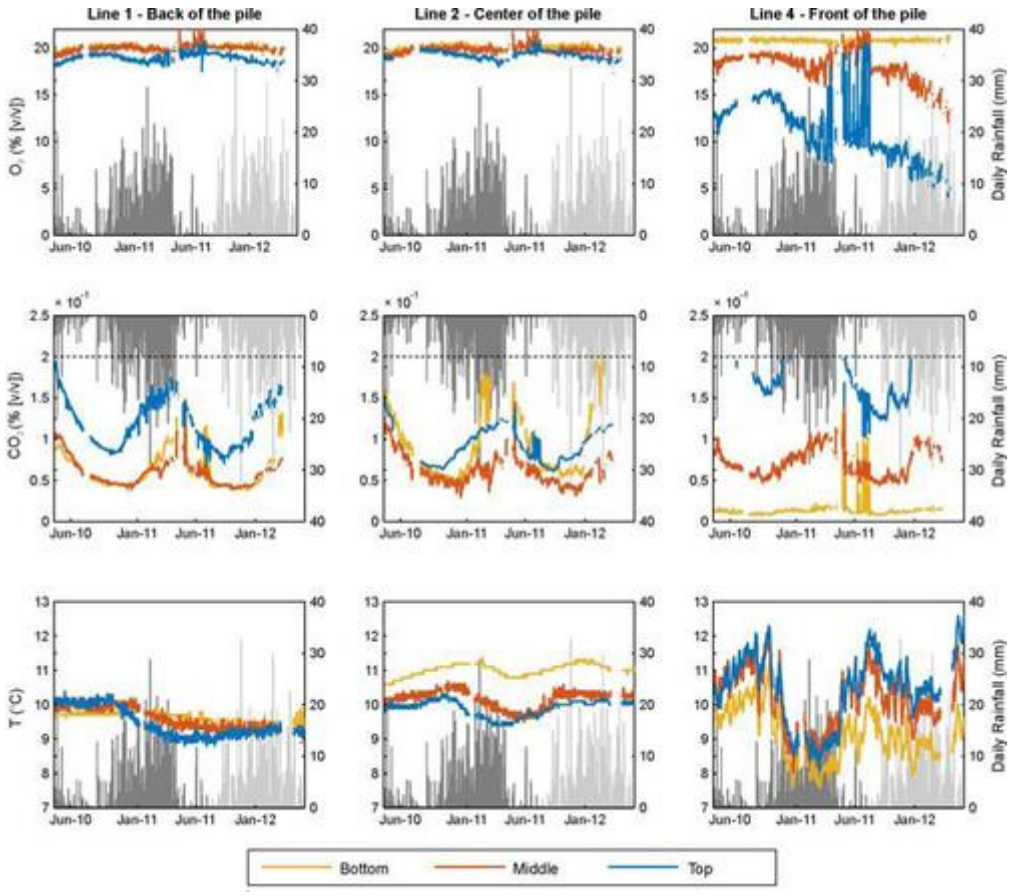

**Figure 5**

Evolution of $O_2$, $CO_2$, and temperature (*T*) with time at selected locations in Instrumentation Lines 1, 2, and 4. The $CO_2$ instrument upper detection limit is 2% (v/v), marked with a dashed black line. For precipitation in the background, dark gray corresponds to data from study site rain gauge, while light gray corresponds to data from a weather station located 4 km away from the site.

The observed $CO_2$ concentrations were generally inversely related to the $O_2$ concentrations, with a substantial buildup of $CO_2$ during the wet season, in particular near the front of the pile, and recovery closer to atmospheric conditions during the dry season. Notably, the range of the $CO_2$ sensor (0–2% [v/v]) was exceeded locally (Line 4, top), implying that $CO_2$ concentrations increased to levels >2% (v/v) in this region. The middle port of Line 1 showed $CO_2$ levels <1% (v/v) during the dry season, but higher concentrations were approached toward the end of the wet season. The $CO_2$ concentrations during the period of humidity buildup (April–July 2011) seem less affected than $O_2$ concentrations, which is probably due to the fact that the infrared-based $CO_2$ measurement is independent of pressure in the sampling tubes.

All $ECH_2O$-TE probes recorded internal temperatures well above the average yearly atmospheric temperature (5.0°C), with the highest temperatures occurring during the end of the dry season. The front of the pile (Line 4) was warmest during the dry season, while temperature increases in the bottom rear of the pile were more moderate. During the wet season, the interior of the pile continued to maintain warmer than ambient temperatures, while the exterior of the pile was cooler, yet still remained at temperatures slightly higher than mean ambient. The largest temperature fluctuations were observed in Line 4, with absolute values ranging from peaks of 12°C (the highest temperature reached in the pile) during dry seasons to near-average air temperatures during the wet season.

The **Fig. 6** cross-plots depict the correlation of $O_2$, $CO_2$, and temperature with VWC. The VWC varied little at the two ports located in the back and center of the pile (L1 middle and L2 bottom, respectively), whereas there were larger variations at the two ports located near the top and front of the pile (L2 top and L4 top, respectively), where the finer material is located.

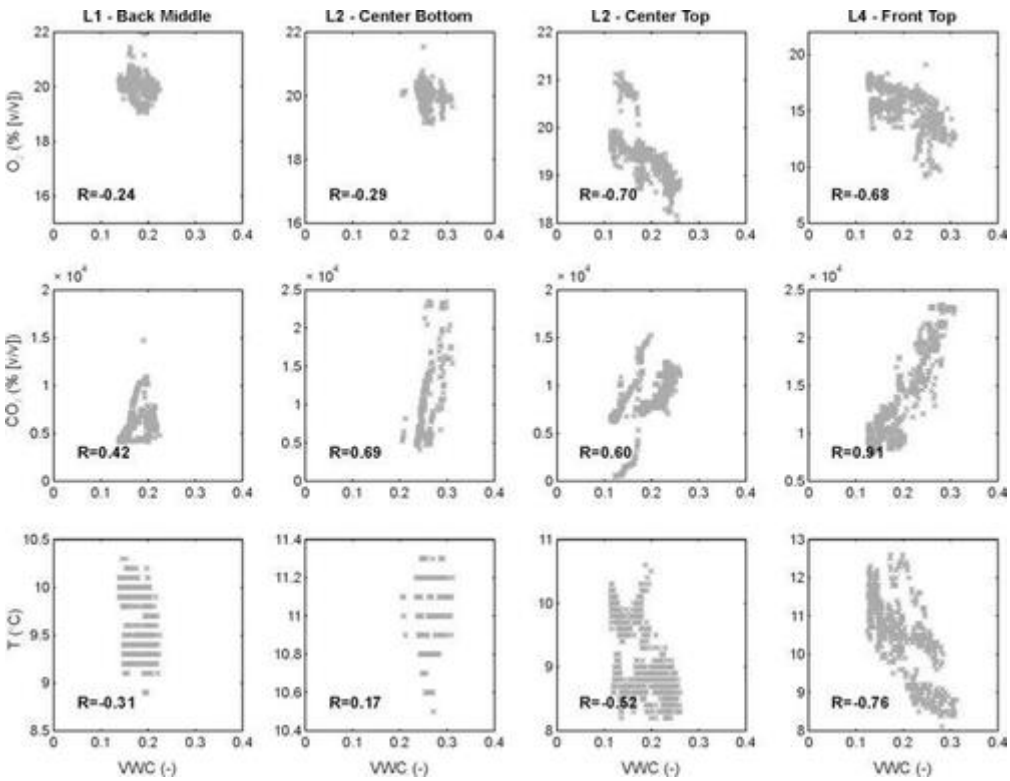


**Figure 6**

Correlation with respect to volumetric water content (VWC) of the ports of Pile 2: L1 middle and L2 bottom are located in the interior of the pile, and L2 top and L4 top are located just below the surface of the pile.

There was a relatively strong positive correlation between $CO_2$ and VWC for all ports, in particular for Port L4 top (front of the pile). Even Port L1 middle (back of the pile) revealed a positive correlation between $CO_2$ concentration and VWC, despite the fact that neither of the two parameters showed a wide range. The $O_2$ content varied little in the interior locations, but larger variations near the front and top of the pile revealed a strong negative correlation between $O_2$ and VWC (L2 top center and L4 top front).

The interior locations showed small temperature fluctuations, and there was no discernable correlation with VWC; however, VWC and temperature were negatively correlated for ports located closer to the external surface of the pile. This was also visually observed in the time series; as soon as the VWC increased at the exterior ports, the temperature decreased (**Fig. 5**).

## Discussion

### Seasonal Influences

Elevated VWCs during the wet season play a major role in the overall geochemical behavior of the experimental pile. Both $O_2$ and $CO_2$ showed marked responses to changes in the VWC (**Fig. 6**), in particular for the locations closer to the pile surface (**Fig. 3**–**5**). During the wet season the VWC increased, which reduced the gas-filled pore space. The increase in VWC therefore inhibits gas migration through the pile, making it more

difficult for $O_2$ to ingress into the pile to sustain sulfide mineral oxidation and for $CO_2$ produced by carbonate mineral dissolution to egress from the pile. These processes explain the observed seasonal variations in gas composition. Notably, this inhibition is independent of the transport mechanism (advection, convection, or diffusion) because a decrease in volumetric gas content reduces both effective gas permeability as well as effective gas diffusion coefficients (**19**; **21**). The strong seasonal climate at the site clearly reveals the importance of the VWC on gas-migration dynamics in waste-rock dumps.

Pile internal temperatures are generally elevated by 3 to 4°C above the mean annual air temperature, which can be attributed to the exothermic nature of sulfide mineral oxidation (**29**). However, in addition to the generally elevated temperatures, seasonal temperature fluctuations can also be observed. In the exterior regions of the waste-rock pile, the temperatures were typically most elevated during the dry season, while temperatures observed during the wet season were closer to atmospheric (**Fig. 3**–**5**). Due to the geographic location of the site, the average ambient air temperatures do not vary significantly during a year (5.1°C in the dry season and 4.9°C in the wet season). Therefore, air temperature fluctuations alone are unlikely to lead to the strong observed temperature variations (up to 4°C) in the exterior regions of the waste-rock pile (**Fig. 5**). Alternatively, these temperature fluctuations can be postulated as driven by seasonal variations in radiative heating. However, average solar radiation at the site also does not change significantly between seasons (9.3 MJ $m^{-2}$ $d^{-1}$ in the dry season and 9.0 MJ $m^{-2}$ $d^{-1}$ in the wet season, based on a multiyear data set for April 2007–March 2011). As a result, variations in ground surface heating are an unlikely source of the observed temperature fluctuations. Seasonal cooling during the wet season may be dominated by the infiltration of cold meteoric water, possibly enhanced by energy loss from evaporation (e.g., **28**). Together, these observations suggest that a more detailed analysis of seasonal temperature fluctuations is warranted based on thermal hydrologic modeling; however, such an exercise was beyond the scope of this study. The observed cooling process is only effective near the surface of a pile and will not be active in a larger scale dump at greater depth.

End-Dumping Segregation

The experimental data indicate that segregation of the material during end dumping affects the pore-gas composition, resulting in $O_2$ and $CO_2$ concentrations that remain similar to atmospheric conditions in the coarse-grained basal layer (**Fig. 3**–**5**), while pore gas near the top of the pile tends to be depleted in $O_2$ and enriched in $CO_2$. This behavior is particularly evident at the front of the experimental pile (Line 4, **Fig. 5**). The particle size distribution in the waste-rock pile is a result of the segregation that occurs during end dumping (**32**; **34**). Finer grained particles that come to rest near the top of the pile are typically characterized by a higher moisture retention capacity inhibiting gas transport (**23**) but also have a higher reactivity due to larger mineral surface areas per unit volume of rock (**1**), increasing $O_2$ consumption and $CO_2$ release. In tandem, these characteristics explain the observed

$O_2$ depletion and $CO_2$ enrichment near the top of the pile. In contrast, the bottom part of the pile remains aerated because of lower material reactivity and greater gas permeability and diffusivity in the basal layer. Both $O_2$ and $CO_2$ can migrate more easily within this layer, while $O_2$ consumption and $CO_2$ generation are more limited. Field observations showed that this was true for the sampling ports located in Lines 1, 2, and 4 (**Fig. 3** and **4**) but not for Line 6 (**Fig. 4**). However, the behavior of Line 6 was a result of pile construction. It has to be kept in mind that Line 6 is located within the protective layer (TP 0), which was not emplaced by end dumping and therefore contains higher proportions of finer grained material. Because this layer is close to the base of the pile, VWCs become more elevated than would occur without this layer, in particular during the wet season. In summary, these data indicate that $O_2$ ingress into the experimental pile is complex and is not simply controlled by diffusion from the surface of the pile toward its center. Vertical concentration profiles for $O_2$ demonstrate that $O_2$ is supplied to surficial waste-rock layers not only from the top of the pile but also by lateral ingress and upward migration. Migration along this pathway can occur by diffusion but is possibly accelerated by advective or convective transport mechanisms due to the higher permeability in the basal region of the pile. The same conclusion is valid for $CO_2$, which egresses toward the surface but also migrates downward into the base of the pile.

## Physical and Chemical Heterogeneity within the Pile

In addition to material heterogeneity introduced by end dumping, physical heterogeneity can be introduced due to differences in material characteristics between the tipping phases. The waste-rock placed during TP 3 is significantly finer grained than the material placed during the two preceding tipping phases (TP 1 and TP 2). In addition, this waste rock also has a local sulfide content of 1.6% (w/w), which is larger than the pile average (about 1.2% [w/w]). The combination of both factors explains the elevated temperatures, decreased $O_2$ concentrations, and increased $CO_2$ concentrations at this location in the pile. Observed temperatures and pore-gas compositions suggest that sulfide oxidation rates are faster in this part of the pile than in waste rock emplaced by the other tipping phases. **25** showed that water collected from the lysimeter just below TP 3 material is characterized by a lower pH and higher $SO_4$ release than the rest of the pile, confirming elevated oxidation rates within this region.

In summary, the combined effects of the physical and chemical heterogeneity of waste rock can lead to hotspots within a waste-rock pile. Gas and temperature data clearly indicate hotspot formation near the front and top of the pile, with inward $O_2$ gradients, outward $CO_2$ gradients, and locally elevated temperatures (**Fig. 3**). Hotspots of similar nature were also observed by **34**. Hotspots are likely to form in physically and chemically heterogeneous full-scale waste-rock dumps, leading to complex gas migration patterns and temperature distributions. These observations are consistent with the numerical simulations by **13**, who demonstrated the importance of heterogeneity on fluid flow and gas transport processes in waste-rock piles.

## Gas Transport Mechanisms

At first sight, the gas-concentration patterns observed in our experimental waste-rock pile with a high level of $O_2$ depletion and $CO_2$ accumulation near the top of the pile and in hotspots (**Fig. 3** and **4**) are not indicative of a diffusive transport mechanism. However, the physical and chemical heterogeneity of the pile must be taken into consideration when interpreting these data. Locally high levels of sulfide oxidation due to abundant sulfide minerals and/or small grain size can lead to local consumption of $O_2$ and buildup of $CO_2$. Vertical downward diffusion into the most reactive and finer grained material from the upper surface of the pile together with lateral diffusion into the less reactive and coarse-grained base of the pile and subsequent upward diffusion can possibly provide an explanation for the observed concentration patterns. Gas diffusion is therefore an important transport mechanism for the experimental waste-rock pile under investigation, in particular for the upper section of the pile and for gas migration into reaction hotspots.

In addition, it is also likely that temperature-induced convection contributes to gas transport into the waste-rock pile. Convection is driven by the internal heating of the pile due to the exothermic nature of sulfide mineral oxidation, which decreases gas density and leads to upward movement (**15**). As a result, air is drawn into the basal regions of the pile, resulting in higher $O_2$ concentrations near the base of the pile than near the top of the pile. These concentration patterns are consistent with our observations and have been observed in several previous field investigations. For example, **12** studied a reclaimed coal mine spoil and found higher $O_2$ concentrations toward the bottom of several boreholes (5–12 m below ground surface) than observed toward the surface. **10** also observed elevated $O_2$ concentrations in some boreholes at the bottom of a dump and attributed it to the role of convection transporting fresh air deep into the dump. Although temperature increases in our experimental piles were relatively limited and the dimensions of the pile are much smaller than those of a full-scale waste-rock pile, it is possible that convection also contributed to gas ingress under these conditions. **16** demonstrated the occurrence of convection for low-permeability material with limited temperature increases, even for a limited pile height. In addition, **14** showed that convection can occur even in cold and covered piles. However, the fine-grained nature and relatively high moisture content of the uppermost waste-rock layer, which includes the traffic surface, inhibits the development of convection cells and therefore limits the contribution of convective gas transport (**16**).

Advective gas transport induced by pressure gradients due to barometric pressure fluctuations may also contribute to gas ingress into the experimental pile investigated, in particular through the higher permeability basal layer (**2**). Barometric pressure fluctuations tend to lead to gas flux into the pile during periods of rising atmospheric pressure and gas egress during periods of falling atmospheric pressure. However, on the scale of our experimental waste-rock pile, barometric pressure fluctuations can only influence gas exchange within the exterior regions of the pile. Analysis shows that for a pressure increase of 3000

Pa (30 mbar), atmospheric air can only penetrate the outermost 0.5 m of the pile, taking into consideration the elevation of the mine site and the pile thickness of 10 m. However, gas advection induced by wind may contribute more significantly to gas migration into and through the pile (**2**).

In summary, based on the analysis conducted, it is not possible to identify a dominant transport mechanism based on gas-concentration data alone. However, our data suggest that diffusion, convection, as well as wind-induced advection probably contribute to $O_2$ ingress into and $CO_2$ egress from the experimental pile. These processes are strongly affected by the physical and chemical heterogeneities of the pile, as discussed above.

Intrinsic Oxidation Rates

Although multiple transport mechanisms probably contribute to gas migration through the pile, it is possible to obtain first-order estimates for intrinsic oxidation rates using a simple one-dimensional diffusion model (**30**), constrained by the observed concentration patterns and VWCs within the pile. To this extent, we investigated two migration pathways into the pile (**Fig. 7**): vertical ingress across the top of the pile to a depth of 2 m, where minimum $O_2$ concentrations were observed (about 10% [v/v] in the wet season for L4 and about 14% [v/v] for the dry season; **Fig. 3**–**5**) and lateral ingress near the bottom and into the core of the pile, where $O_2$ concentrations showed only a small depletion relative to atmospheric values year-round (about 20% [v/v]; **Fig. 3**–**5**).

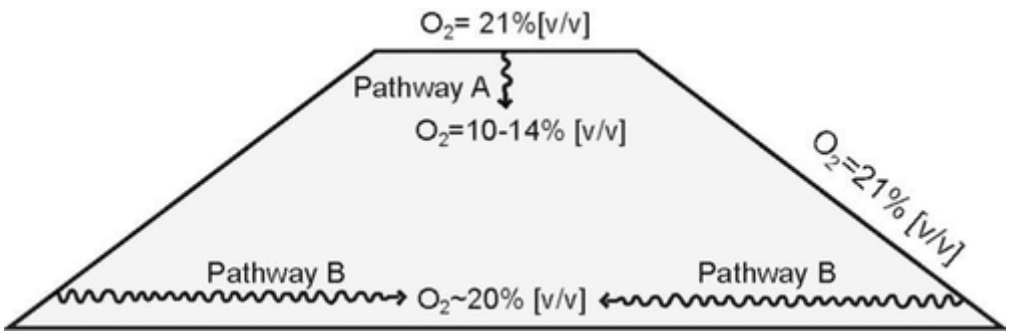


**Figure 7**

View of the experimental pile from the front, with the conceptual model for the numerical analysis. Exterior boundary 21% (v/v) $O_2$ and two pathways analyzed were based on the assumption that the gas supply is diffusion controlled.

Assuming that diffusion is the only $O_2$ supply mechanism, the effective oxidation rate depends only on the concentration of $O_2$ in the pore gas, being equal to the intrinsic oxidation rate ($S_o$) when the concentration is equal to the atmospheric concentration. A one-dimensional diffusion model with a sink for $O_2$ consumption throughout the domain can be used to describe this system (30):

$$D_{\text{eff}}\frac{\partial^2 C}{\partial x^2} = \frac{S_o}{C_o}C \quad (3)$$

where $D_{eff}$ is the effective diffusion coefficient, $C$ is the $O_2$ concentration as a function of migration distance $x$, and $C_o$ is the concentration of $O_2$ in the atmosphere. Assuming that the concentration at the surface boundary, $C_o$, is constant and there is no flux across the interior boundary of the domain (Fig. 7), the analytical solution for Eq. [3] is (30)

$$C(x) = C_o \frac{\cosh[\varepsilon(x-1)]}{\cosh\varepsilon} \quad (4)$$

where

$$\varepsilon = \sqrt{\frac{h^2 S_o}{D_{eff} C_o}} \quad (5)$$

In this solution, the spatial coordinate $x$ has been normalized with $x = 0$ located at the exterior of the domain and $x = 1$ at the interior symmetry boundary. The spatial dimensions of the transport pathways are taken into consideration through the variable $h$, which represents the actual distance between interior and exterior boundaries.

To apply the model, effective diffusion coefficients were estimated as a function of gas-filled pore space and porosity. The relationship between effective diffusion coefficients and soil properties has been studied by several researchers (for example, **21**). Two common models (**20** and **19**) were used in this study to estimate the effective diffusion coefficients constrained by the observed VWCs for both wet and dry seasons (**Fig. 2**). In general, gas diffusion coefficients in waste rock are higher than those predicted by these two models (**15**; **29**). Therefore, the linear model proposed by **27** was also used to estimate $D_{eff}$. Based on these diffusion coefficients, the model was calibrated by adjusting the intrinsic oxidation rate to match the observed concentration gradients for both migration pathways under both wet and dry conditions. Effective diffusion coefficients and the range of calibrated oxidation rates are provided in **Table 3**. The simulation results are graphically presented in **Fig. 8a** for the case using diffusion coefficients based on the model of **27**. As observed in the data, the model predicts lower $O_2$ concentrations in the wet season.

**Table 3.** Parameters used for the diffusion model: porosity ($\phi$), volumetric gas content ($\theta_g$), effective diffusivity ($D_{eff}$) according to three models, and $O_2$ consumption rate ($S_o$).

| **Position in pile and season** | **$\phi$** | **$\theta_g$** | **$D_{eff}$†** | | | **$S_o$** |
|---|---|---|---|---|---|---|
| | | | 20 | 19 | 15 | |
| | | | $m^2\ s^{-1}$ | | | kg $O_2$ $m^{-3}$ $s^{-1}$ |
| Top, dry | 0.33 | 0.25 | $2.0 \times 10^{-6}$ | $1.9 \times 10^{-6}$ | $4.5 \times 10^{-6}$ | $4.8 \times 10^{-8}$–$1.1 \times 10^{-7}$ |

| **Position in pile and season** | **$\phi$** | **$\theta_g$** | **$D_{eff}$†** | | | **$S_o$** |
|---|---|---|---|---|---|---|
| | | | 20 | 19 | 15 | |
| Top, wet | 0.33 | 0.08 | $1.2 \times 10^{-7}$ | $4.3 \times 10^{-8}$ | $1.5 \times 10^{-6}$ | $3.4 \times 10^{-9}$–$1.2 \times 10^{-7}$ |
| Bottom, dry | 0.35 | 0.27 | $2.3 \times 10^{-6}$ | $2.2 \times 10^{-6}$ | $4.9 \times 10^{-6}$ | $1.3 \times 10^{-10}$–$2.9 \times 10^{-10}$ |
| Bottom, wet | 0.35 | 0.17 | $7.3 \times 10^{-7}$ | $4.7 \times 10^{-7}$ | $3.1 \times 10^{-6}$ | $6.1 \times 10^{-11}$–$4.0 \times 10^{-10}$ |

- † 20: $D_{eff} = \theta_g^{3/2}(\theta_g/\phi)D_o$, 19: $D_{eff} = \theta_g^{4/3}(\theta_g/\phi)^2 D_o$, 27: $D_{eff} = 0.85\theta_g D_o$, where $D_o$ is the $O_2$ diffusion coefficient in air ($2.13 \times 10^{-5}$ m$^2$ s$^{-1}$).

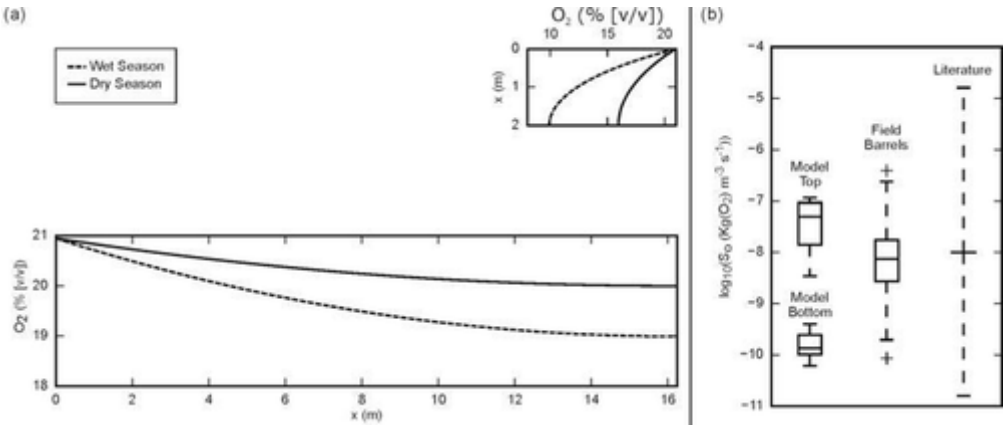


**Figure 8**

(a) Calibrated model results for wet and dry season $O_2$ concentration for the top (Pathway A) and bottom (Pathway B) of the experimental pile presented on top of a half-pile view, and (b) calibrated intrinsic oxidation rates obtained from the analytical model compared with oxidation rates derived from $SO_4$ release rates from field barrels containing the same rock types (**7**) and the range of intrinsic oxidation rates reported in the literature (**5**; **29**). The model simulations provide first-order estimates of intrinsic reaction rates solely based on a diffusion-dominated $O_2$–supply mechanism.

**Figure 8b** summarizes the calibrated intrinsic oxidation rates for both regions in the pile as box plots and provides a comparison with literature values and experimental data from the mine site derived from field-barrel tests. For each calculation, $D_{eff}$ was calculated based on the three tortuosity models (**Table 3**). The length of the pathway was fixed and $S_o$ was modified to match the measured $O_2$ concentrations for each season at the interior boundary (10% [v/v] for top wet, 14% [v/v] for top dry, 19% [v/v]for bottom wet, and 20% [v/v] for bottom dry). Calibrated intrinsic oxidation rates near the top of the pile ranged from $3.4 \times 10^{-9}$ to $1.2 \times 10^{-7}$ kg $O_2$ m$^{-3}$ s$^{-1}$, while the corresponding rates for the basal region of the pile ranged from $6.1 \times 10^{-11}$ to $4 \times 10^{-10}$ kg $O_2$ m$^{-3}$ s$^{-1}$.

These calibrated rates fall into the broad range of literature values, varying between $10^{-5}$ and $10^{-11}$ kg $O_2$ $m^{-3}$ $s^{-1}$ (**5**; **29**). More importantly, the calibrated intrinsic oxidation rates can also be compared with oxidation rates derived from field-barrel experiments composed of the same waste rock as was used for the pile, based on weekly $SO_4$ release rates (**7**). These oxidation rates showed a narrower range from $10^{-7}$ to $10^{-10}$ kg $O_2$ $m^{-3}$ $s^{-1}$. Additional details on the experimental setup of the field barrels were provided by **7**.

Calibrated intrinsic oxidation rates for the finer grained material near the top fall in the higher range of rates derived from the field barrels, while rates for the basal layer are near the lower range of rates for the field barrels. Differences between the intrinsic oxidation rates at the different locations are probably affected by the more reactive nature of the smaller sized material near the top compared with the coarser material placed at the bottom of the pile.

The one-dimensional reaction–diffusion model provides a simple approach to estimate reasonable intrinsic oxidation rates for the finer grained material near the top of the pile, further confirming that diffusion is an important (if not dominating) gas transport process in this region of the pile. However, the fact that calibrated intrinsic oxidation rates for the base of the pile are relatively low may be an artifact of applying the diffusion model rather than a model with a more complete mechanistic formulation (**15**; **6**; **22**). Higher rates could be obtained if advection and/or convection were incorporated into the model. These findings suggest that convective and/or advective gas transport, probably wind induced, may contribute to the $O_2$ supply into the pile.

**Summary and Conclusions**

For this study, we characterized the pore-gas composition ($CO_2$ and $O_2$), internal temperature, and VWC in a 10-m-high experimental sulfidic waste-rock pile exposed to natural weathering conditions. We monitored the spatial distribution of these parameters and their temporal fluctuations for a time period of 2 yr.

The results show a strong effect of seasonal climate variations on the hydrological response, temperature, and gas composition of the pile. During the wet season, as the internal VWC increased, the pore-gas composition deviated further from the atmospheric gas composition than it did during the dry season. Increased VWC inhibited gas exchange with the atmosphere and lead to a significant depletion of $O_2$ and enrichment of $CO_2$ within sections of the pile. In addition, a pronounced cooling effect was seen near the surface of the pile, which may be due to the infiltration of cold meteoric water, which overprints heat generation from sulfide oxidation.

Gas composition is affected by the material segregation caused by end dumping and the presence of a traffic surface at the top of the pile, which leaves finer grained and more reactive material near the top of the pile and coarser grained rock with lower reactivity at the base of the pile. The combined effect of this structural heterogeneity led to the highest level of $O_2$ depletion and $CO_2$ enrichment near the surface of the

pile, while pore gas in intermediate and basal waste-rock layers remained generally closer to atmospheric conditions.

In addition to this structural heterogeneity, material-related physical and chemical heterogeneities also affected the pore-gas composition. The construction of the pile in separate tipping phases led to the placement of distinct material types with different grain sizes, sulfide contents, and reactivity. Data on $O_2$, $CO_2$, and temperature show that the front of the pile is the most reactive zone, forming a hotspot of oxidative weathering.

An assessment of the transport mechanisms based on the observational data suggests that diffusion is an important, if not dominant, transport process in the upper region of the pile, which is characterized by small grain size, low permeability, and high reactivity. However, it is likely that convection and wind-induced advection also contribute to gas transport, in particular in the coarse-grained basal region of the pile with higher permeability. Using a simple diffusion model, two one-dimensional diffusion pathways were modeled to obtain first-order estimates of intrinsic oxidation rates within the pile. The calibrated rates obtained for the top of the experimental pile ($3.4 \times 10^{-9}$–$1.2 \times 10^{-7}$ kg $O_2$ $m^{-3}$ $s^{-1}$) were two to three orders of magnitude larger than the ones obtained for the basal layer (bottom of the pile; $6.1 \times 10^{-11}$–$4 \times 10^{-10}$ kg $O_2$ $m^{-3}$ $s^{-1}$), indicating a strong effect of pile structure and grain size distribution with depth on reactivity. Overall, the rates fall in the range of intrinsic oxidation rates estimated for full-scale waste-rock piles at other sites and are consistent with rate estimates from field barrel tests at this site, despite the difference in experimental scale. The relatively low intrinsic oxidation rates obtained for the basal region of the pile were probably affected by the simplified nature of the modeling approach and indicate that gas convection and/or advection might play a role in supplying $O_2$ into this more permeable layer.

This work represents a 2-yr window into processes occurring in an experimental waste-rock pile, also providing valuable insights for waste-rock weathering on a larger scale. Many of the features observed at the experimental scale should be relevant for full-scale dumps, possibly in an amplified manner, considering that heterogeneity is greater due to the placement of many different rock types, because grain-size segregation by end dumping increases with tipping face length, and because internal temperatures will be warmer due to larger volume/surface ratios. We expect that full-scale traffic surfaces and the associated compaction will also have important effects on the overall gas transport in full-scale storage facilities.

**Acknowledgments**

Funding for this study was provided by the Natural Sciences and Engineering Research Council of Canada (NSERC) through the Collaborative Research and Development (CRD) program with industrial funding from Teck Resources. The work was also supported by Compañía Minera Antamina S.A. Additional funding for the $O_2$ and $CO_2$ gas analysis system was provided by

the Canada Foundation for Innovation (CFI) through the Leaders of Opportunity Fund (LOF). Maria E. Lorca was supported through a scholarship from Comisión Nacional de Investigación Científica y Tecnológica de Chile (CONICYT). We would like to thank Celedonio Aranda, Edsael Sanchez, Alexander Robles, and Bartolome Vargas for technical and logistical support at the mine site. In addition, we would like to thank Holly Peterson, Sharon Blackmore, Trevor Hirsche, and Mehrnoush Javadi for assistance in the field. We also would like to acknowledge Olga Singurindy's contributions during early phases of this study.

References

1Amos, R.T., Blowes, D.W., Bailey, B.L., Sego, D.C., Smith, L., and Ritchie, A.I.M. 2015. Waste-rock hydrogeology and geochemistry. Appl. Geochem. 57: 140– 156. https://doi.org/10.1016/j.apgeochem.2014.06.020 http://gateway.webofknowledge.com/gateway/Gateway.cgi?GWVersion=2&SrcApp=PARTNER_APP&SrcAuth=Agronomy_sub&KeyUT=WOS:000354283200011&DestLinkType=FullRecord&DestApp=WOS_CPL&UsrCustomerID=9992b2403adf8c36119d0b6fce39b97c

Google Scholar

2Amos, R.T., Blowes, D.W., Smith, J.L., and Sego, D.C. 2009. Measurement of wind-induced pressure gradients in a waste rock pile. Vadose Zone J. 8: 953– 962. https://doi.org/10.2136/vzj2009.0002 http://gateway.webofknowledge.com/gateway/Gateway.cgi?GWVersion=2&SrcApp=PARTNER_APP&SrcAuth=Agronomy_sub&KeyUT=WOS:000271936900013&DestLinkType=FullRecord&DestApp=WOS_CPL&UsrCustomerID=9992b2403adf8c36119d0b6fce39b97c

Google Scholar

3Bakker, M., and Nieber, J.L. 2009. Damping of sinusoidal surface flux fluctuations with soil depth. Vadose Zone J. 8: 119– 126. https://doi.org/10.2136/vzj2008.0084 http://gateway.webofknowledge.com/gateway/Gateway.cgi?GWVersion=2&SrcApp=PARTNER_APP&SrcAuth=Agronomy_sub&KeyUT=WOS:000263915100012&DestLinkType=FullRecord&DestApp=WOS_CPL&UsrCustomerID=9992b2403adf8c36119d0b6fce39b97c

Google Scholar

4Bay, D.S., Peterson, H.E., Singurindy, O., Aranda, C.A., Dockrey, J.W., and Sifuentes Vargas, F. et al. 2009. Assessment of neutral pH drainage from three experimental waste-rock piles at the Anta-Mina mine, Peru. In: Proceedings of the 8th International Conference on Acid Rock Drainage and Securing the Future: Mining, Metals & the Environment in a Sustainable Society, Skellefteå, Sweden. 22–26 June 2009. Vol. 1. Swedish Assoc. Mines, Miner., Metal Prod., Stockholm. p. 188– 199.

Google Scholar

5Bennett, J.W., Comarmond, M.J., and Jeffery, J.J. 2000. Comparison of sulfidic oxidation rates measured in the laboratory and the field. In: Proceedings of the Fifth International Conference on Acid Rock Drainage, ICARD 2000, Denver, CO. 21–24 May 2000. Soc. Min., Metall., Explor., Englewood, CO. p. 171– 180.

Google Scholar

6Binning, P.J., Postma, D., Russell, T.F., Wesselingh, J.A., and Boulin, P.F. 2007. Advective and diffusive contributions to reactive gas transport during pyrite oxidation in the unsaturated zone. Water Resour. Res. 43: W02414. https://doi.org/10.1029/2005WR004474

Google Scholar

7Blackmore, H.E. 2015. The role of hydrology, geochemistry and microbiology in flow and solute transport through highly heterogeneous, unsaturated waste rock at various test scales. Ph.D. diss. Dep. of Earth,

Ocean and Atmospheric Sciences, Univ. of British Columbia, Vancouver, BC, Canada.

Google Scholar

8Chi, X., Amos, R.T., Stastna, M., Blowes, D., Sego, D., and Smith, L. 2013. The Diavik Waste Rock Project: Implications of wind-induced gas transport. Appl. Geochem. 36: 246– 255. https://doi.org/10.1016/j.apgeochem.2012.10.015 http://gateway.webofknowledge.com/gateway/Gateway.cgi?GWVersion=2&SrcApp=PARTNER_APP&SrcAuth=Agronomy_sub&KeyUT=WOS:000323939600021&DestLinkType=FullRecord&DestApp=WOS_CPL&UsrCustomerID=9992b2403adf8c36119d0b6fce39b97c

Google Scholar

9Fala, O., Molson, J., Aubertin, M., and Bussière, B. 2005. Numerical modelling of flow and capillary barrier effects in unsaturated waste rock piles. Mine Water Environ. 24: 172– 185. https://doi.org/10.1007/s10230-005-0093-z

Google Scholar

10Harries, J.R., and Ritchie, A.I.M. 1985. Pore gas composition in waste rock dumps undergoing pyritic oxidation. Soil Sci. 140: 143– 152. https://doi.org/10.1097/00010694-198508000-00010

Google Scholar

11Javadi, M., Peterson, H., Blackmore, S., Mayer, K.U., Beckie, R.D., and Smith, L. 2012. Evaluating preferential flow in an experimental waste rock pile using unsaturated flow and solute transport modeling. In: W.A. Price, editor, Proceedings of the 9th International Conference on Acid Rock Drainage, Ottawa, ON, Canada. 20–26 May 2012. Vol. 2. Curran Assoc., Red Hook, NY. p. 1210– 1219.

Google Scholar

12Jaynes, D., Rogowski, A., Pionke, H., and Jacoby, E. 1983. Atmosphere and temperature changes within a reclaimed coal strip mine. Soil Sci. 136: 164– 177. https://doi.org/10.1097/00010694-198309000-00004

Google Scholar

13Lahmira, B., Lefebvre, R., Aubertin, M., and Bussière, B. 2016. Effect of heterogeneity and anisotropy related to the construction method on transfer processes in waste rock piles. J. Contam. Hydrol. 184: 35– 49. https://doi.org/10.1016/j.jconhyd.2015.12.002 http://gateway.webofknowledge.com/gateway/Gateway.cgi?GWVersion=2&SrcApp=PARTNER_APP&SrcAuth=Agronomy_sub&KeyUT=WOS:000370768400004&DestLinkType=FullRecord&DestApp=WOS_CPL&UsrCustomerID=9992b2403adf8c36119d0b6fce39b97c

Google Scholar

14Lahmira, B., Lefebvre, R., Hockley, D., and Phillip, M. 2014. Atmospheric controls on gas flow directions in a waste rock dump. Vadose Zone J. 13(10). https://doi.org/10.2136/vzj2014.03.0032

Google Scholar

15Lefebvre, R., Hockley, D., Smolensky, J., and Gélinas, P. 2001a. Multiphase transfer processes in waste rock piles producing acid mine drainage: 1. Conceptual model and system characterization. J. Contam. Hydrol. 52: 137– 164. https://doi.org/10.1016/S0169-7722(01)00156-5

Google Scholar

16Lefebvre, R., Hockley, D., Smolensky, J., and Lamontagne, A. 2001b. Multiphase transfer processes in waste rock piles producing acid mine drainage: 2. Applications of numerical simulation. J. Contam. Hydrol. 52: 165– 186. https://doi.org/10.1016/S0169-7722(01)00157-7

Google Scholar

17Linklater, C.M., Sinclair, D.J., and Brown, P.L. 2005. Coupled chemistry and transport modelling of sulphidic waste rock dumps at the Aitik mine site, Sweden. Appl. Geochem. 20: 275– 293. https://doi.org/10.1016/j.apgeochem.2004.08.003

Google Scholar

18Lundgren, T. 2001. The dynamics of oxygen transport into soil covered mining waste deposits in Sweden. J. Geochem. Explor. 74: 163– 173. https://doi.org/10.1016/S0375-6742(01)00182-0

Google Scholar

19Millington, R., and Quirk, J. 1961. Permeability of porous solids. Trans. Faraday Soc. 57: 1200– 1207. https://doi.org/10.1039/tf9615701200

Google Scholar

20Moldrup, P., Olesen, T., Gamst, J., Schjønning, P., Yamaguchi, T., and Rolston, D.E. 2000. Predicting the gas diffusion coefficient in repacked soil. Soil Sci. Soc. Am. J. 64: 1588– 1594. https://doi.org/10.2136/sssaj2000.6451588x

Google Scholar

21Moldrup, P., Olesen, T., Komatsu, T., Schjønning, P., and Rolston, D.E. 2001. Tortuosity, diffusivity, and permeability in the soil, liquid and gaseous phases. Soil Sci. Soc. Am. J. 65: 613– 623. https://doi.org/10.2136/sssaj2001.653613x

Google Scholar

22Molins, S., and Mayer, K.U. 2007. Coupling between geochemical reactions and multicomponent gas and solute transport in unsaturated media: A reactive transport modeling study. Water Resour. Res. 43: W05435. https://doi.org/10.1029/2006WR005206

Google Scholar

23Molson, J.W., Fala, O., Aubertin, M., and Bussière, B. 2005. Numerical simulations of pyrite oxidation and acid mine drainage in unsaturated waste rock piles. J. Contam. Hydrol. 78: 343– 371. https://doi.org/10.1016/j.jconhyd.2005.06.005

Google Scholar

24Pantelis, G., Ritchie, A.I.M., and Stepanyants, Y.A. 2002. A conceptual model for the description of oxidation and transport processes in sulphidic waste rock dumps. Appl. Math. Modell. 26: 751– 770. https://doi.org/10.1016/S0307-904X(01)00085-3

Google Scholar

25Peterson, H.E. 2014. Unsaturated hydrology, evaporation, and geochemistry of neutral and acid rock drainage in highly heterogeneous mine waste rock at the Antamina mine, Peru. Ph.D. diss. Dep. of Earth and Ocean Sciences, Univ. of British Columbia, Vancouver, BC, Canada.

Google Scholar

26Peterson, H., Beckie, R.D., Harrison, B., Mayer, K.U., and Smith, J.L. 2012. Rapid seasonal transition from neutral to acidic drainage in a waste rock test pile at the Antamina mine, Peru. In: W.A. Price, editor, Proceedings of the 9th International Conference on Acid Rock Drainage, Ottawa, ON, Canada. 20–26 May 2012. Vol. 2. Curran Assoc., Red Hook, NY. p. 1220– 1231.

Google Scholar

27Pruess, K. 1991. TOUGH2: A general-purpose numerical simulator for multiphase fluid and heat transfer. Rep. LBL-29400. Lawrence Berkeley Lab., Berkeley, CA.

Google Scholar

28Qiu, G.Y., and Ben-Asher, J. 2010. Experimental determination of soil evaporation stages with soil surface temperature. Soil Sci. Soc. Am. J. 74: 13– 22. https://doi.org/10.2136/sssaj2008.0135 http://gateway.webofknowledge.com/gateway/Gateway.cgi?GWVersion=2&SrcApp=PARTNER_APP&SrcAuth=Agronomy_sub&KeyUT=WOS:000273579100003&DestLinkType=FullRecord&DestApp=WOS_CPL&UsrCustomerID=9992b2403adf8c36119d0b6fce39b97c

Google Scholar

29Ritchie, A.I.M. 2003. Oxidation and gas transport in piles of sulfidic material. In: J.L. Jambor et al., editors, Environmental aspects of mine wastes. Short Course Series. Mineral. Assoc. Canada, Ottawa ON. p. 73–94.

Google Scholar

30Ritchie, A.I.M., and Miskelly, P. 2000. Geometric and physico-chemical properties determining sulfide oxidation rates in waste rock dumps, In: Proceedings of the 5th International Conference on Acid Rock Drainage, ICARD 2000, Denver, CO. 21–24 May 2000. Soc. Min., Metall., Explor., Englewood, CO. p. 277– 287.

Google Scholar

31Singurindy, O., Lorca, M.E., Peterson, H., Hirsche, T., Javadi, M., and Blackmore, S. et al. 2012. Spatial and temporal variations of O2 and CO2 pore gas concentrations in an experiment waste rock pile at the Antamina Mine, Peru. In: W.A. Price, editor, Proceedings of the 9th International

Conference on Acid Rock Drainage, Ottawa, ON, Canada. 20–26 May 2012. Vol. 2. Curran Assoc., Red Hook, NY. p. 1232– 1241.

Google Scholar

32Smith, J.L., and Beckie, R.D. 2003. Hydrologic and geochemical transport processes in mine waste rock. In: J.L. Jambor et al., editors, Environmental aspects of mine wastes. Short Course Series. Mineral. Assoc. Canada, Ottawa, ON. p. 51– 72.

Google Scholar

33Sracek, O., Gelinas, P., Lefebvre, R., and Nicholson, R.V. 2006. Comparison of methods for the estimation of pyrite oxidation rate in a waste rock pile at Mine Doyon site, Quebec, Canada. J. Geochem. Explor. 91: 99– 109. https://doi.org/10.1016/j.gexplo.2006.03.002 http://gateway.webofknowledge.com/gateway/Gateway.cgi?GWVersion=2&SrcApp=PARTNER_APP&SrcAuth=Agronomy_sub&KeyUT=WOS:000241132000007&DestLinkType=FullRecord&DestApp=WOS_CPL&UsrCustomerID=9992b2403adf8c36119d0b6fce39b97c

Google Scholar

34Stockwell, J., Smith, L., Jambor, J.L., and Beckie, R. 2006. The relationship between fluid flow and mineral weathering in heterogeneous unsaturated porous media: A physical and geochemical characterization of a waste-rock pile. Appl. Geochem. 21: 1347– 1361. https://doi.org/10.1016/j.apgeochem.2006.03.015 http://gateway.webofknowledge.com/gateway/Gateway.cgi?GWVersion=2&SrcApp=PARTNER_APP&SrcAuth=Agronomy_sub&KeyUT=WOS:000240297600009&DestLinkType=FullRecord&DestApp=WOS_CPL&UsrCustomerID=9992b2403adf8c36119d0b6fce39b97c

Google Scholar

35Wels, C., Lefebvre, R., and Robertson, A.M. 2003. An overview of prediction and control of air flow in acid-generating waste rock dumps. In: Proceedings of the 6th International Conference on Acid Rock DrainageCairns, North Queensland, Australia. 12–18 July 2003. Australasian Inst. Min. Metall., Carlton South, VIC, Australia. p. 639–650.

Google Scholar

36Zhang, K., Wu, Y.-S., and Pan, L. 2006. Temporal damping effect of the Yucca Mountain fractured unsaturated rock on transient infiltration pulses. J. Hydrol. 327: 235– 248. https://doi.org/10.1016/j.jhydrol.2005.11.023 http://gateway.webofknowledge.com/gateway/Gateway.cgi?GWVersion=2&SrcApp=PARTNER_APP&SrcAuth=Agronomy_sub&KeyUT=WOS:000239671700019&DestLinkType=FullRecord&DestApp=WOS_CPL&UsrCustomerID=9992b2403adf8c36119d0b6fce39b97c